Studies of Proton-Irradiated SO_2 at Low Temperatures: Implications for Io

MARLA H. MOORE[1]

NASA/Goddard Space Flight Center, Greenbelt, Maryland 20771

The infrared absorption spectrum from 3.3 to 27 μm (3030–370 cm^{-1}) of SO_2 ice films has been measured at 20 and 88°K before and after 1-MeV proton irradiation. The radiation flux was chosen to simulate the estimated flux of Jovian magnetospheric 1-MeV protons incident on Io. After irradiation, SO_3 is identified as the dominant molecule synthesized in the SO_2 ice. This is also the case after irradiation of composite samples of SO_2 with sulfur, or disulfites. Darkening was observed in irradiated SO_2 ice and in irradiated S_x pellets. Photometric and spectral measurements of the thermoluminescence of irradiated SO_2 have been made during warming. The spectrum appears as a broad band with a maximum at 4450 Å. Analysis of the luminescence data suggests that, at Ionian temperatures, irradiated SO_2 ice would not be a dominant contributor to posteclipse brightening phenomena. After warming to room temperature, a form of SO_3 remains along with a sulfate and S_x. Based on these experiments, it is reasonable to propose that small amounts of SO_3 may exist on the surface of Io as a result of irradiation synthesis in SO_2 frosts.

INTRODUCTION

A. Observations of Io

The Voyager 1 encounter with Io revealed its colorful terrain. Although Io is perhaps the reddest object in the solar system, it shows large variations in color and albedo over the globe. It is the only object other than Earth which is known to have active volcanos.

Io's deep absorption near 2460 cm^{-1}, measured from ground-based observations, is attributed to the $\nu_1 + \nu_3$ absorption of solid SO_2 (Fanale *et al.*, 1979; Smythe *et al.*, 1979). Condensation of SO_2 is possible on much of Io where surface temperatures are no higher than 135–140°K due to solar heating (bond albedo = 0.6); nighttime temperatures are as low as 90°K. It is postulated that SO_2 is the principal volatile volcanic effluent which condenses on the surface, forming a frost or adsorbate even over regions not associated with volcanic hot spots

(Bertaux and Belton, 1979; Smythe *et al.*, 1979; Fanale *et al.*, 1979; Nelson *et al.*, 1980). Pearl *et al.* (1979) identified gaseous SO_2 (ν_3 absorption near 1350 cm^{-1}) on Io using Voyager 1 IRIS infrared scans of a volcanic feature and its plume; they estimated its abundance to be consistent with an atmosphere of SO_2 in equilibrium with solid SO_2. Observations of Io in the 2900 to 3200 Å region from the Earth-orbiting IUE satellite showed no detectable gaseous SO_2 ultraviolet absorption features (Butterworth *et al.*, 1980). The discrepancy between the lower abundance limit for SO_2 on Io suggested by the IUE data compared with the abundance supported by the Voyager IRIS data is under debate.

Wamstecker *et al.* (1974) first suggested that abundant elemental sulfur may exist on the Ionian surface based on the similarity of the optical reflectivity of Io to that of sulfur. Many of the detailed colorations photographed by Voyager 1 are considered consistent with flows of quenched molten sulfur (e.g., Sagan, 1979). The surface is also expected to have significant quantities of

sodium and potassium, since clouds of sodium and potassium are observed at the orbit of Io (Brown, 1974; Trafton, 1975). The existence of sulfur and oxygen ions coincident with the orbit of Io (Bridge *et al.*, 1979) is additional evidence for the existence of sulfur and oxygen on Io.

B. Ionian Radiation Environment

Io orbits at $5.9R_J$ (R_J = radius of Jupiter = 71,398 km) from Jupiter and its surface is subjected to the relatively intense flux of charged particles in the Jovian magnetosphere. The flux of positive ions was measured near $6R_J$ by the low-energy telescope (LET) experiment on Pioneer 10 (Trainor *et al.*, 1974) and by the low-energy charged-particle (LECP) experiment ($E > 20$ keV nucleon^{-1}) on Voyager I (Krimigis *et al.*, 1979). The relative contributions of different ion species to the flux were not determined by either experiment.

In the present laboratory experiments, the radiation field on Io was simulated using 1-MeV protons; the appropriate magnitude for this ion flux was obtained using an interpretation of the LECP data by Lanzerotti *et al.* (1982). The differential energy spectrum (particles cm^{-2} sec^{-1} MeV^{-1} vs kinetic energy) at $R_J = 6$ was interpolated using data from nearby distances ($5.6R_J$–$9.5R_J$). The energy spectrum has a low-energy roll-over beginning at $E \approx 1$ MeV and decreases at $\sim E^{-4}$ at high energies. Assuming all ions are hydrogen ions, the 1-MeV omnidirectional differential proton flux could be as large as 4×10^5 cm^{-2} sec^{-1} MeV^{-1}. After appropriate integrations ($1.1 < E < 2.1$ MeV), the Voyager 1 value becomes 2×10^5 protons cm^{-2} sec^{-1} MeV^{-1}; this is in reasonable agreement with the Pioneer 10 result of 5.6–6.3×10^5 protons cm^{-2} sec^{-1} MeV^{-1}. For a 1-MeV differential proton flux of 2×10^5 cm^{-2} sec^{-1} MeV^{-1} per hemisphere (the value used in the present experimental simulations) Io would receive 6.3×10^{12} MeV cm^{-2} year^{-1} (referred to hereafter as 1 Ionian dose or 1 ID for convenience).

In addition to the flux of energetic hydrogen ions in the Jovian magnetosphere at $6R_J$, cold plasma ions (E < 6 keV), assumed to be oxygen and sulfur, were measured by the Voyager 1 plasma science (PLS) instrument (Bridge *et al.*, 1979). It is estimated that the flux of these ions (E ~ 0.1 keV) is the order of 100 times that of 1-MeV protons. Another component of the charged-particle radiation in the Jovian magnetosphere is due to the anisotropic electron flux which has been modeled by Divine and Garrett (1983). They predict a 1-MeV omnidirectional differential electron flux of ~4 $\times 10^7$ cm^{-2} sec^{-1} MeV^{-1}.

Some of the expected effects of this relatively intense magnetospheric particle radiation on Io's surface materials include albedo changes, sputtering, radiation-induced luminescence, and molecular synthesis. Studies of the effects of proton radiation on the reflectance spectra of Ionian candidate materials such as sulfur/salt mixtures (Nash and Fanale, 1977; Nelson and Nash, 1979) suggested that radiation darkening may be partly responsible for the albedo differences observed on Io.

The alteration of surface SO₂ frosts on Io by charged-particle erosion has been studied in laboratory sputtering experiments. SO₂-erosion yields have been measured by Lanzerotti *et al.* (1982) as a function of ion energy, ion specie, and ice temperature. It is estimated that at 10°K, ~0.3 SO₂ molecules are sputtered for each 1-MeV proton impact. The erosion of S or O₂, SO, SO₂, and presumably SO₃ (identified from mass spectrometer peaks corresponding to mass 32, 48, 64, and 80, respectively), from keV Ar$^+$-ion bombardment of SO₂ ice films was recently reported by Boring *et al.* (1983) and Johnson *et al.* (1984). They estimate that an equilibrium concentration of 1 or 2% SO₃ could be synthesized in the top few monolayers of SO₂ ice on Io as the result of low-energy ion bombardment. The erosion rate of fresh SO₂ deposits due to sputtering is of the order of 10 μm per years. Melcher *et al.* (1982) reported that an oxygen-rich

residue remained after warming irradiated SO_2 ice. The erosion rate of this residue was estimated to be about a factor of 10 less than that of SO_2 at 10°K.

The phenomenon of posteclipse brightening has been reported (Binder and Cruikshank, 1964). They found that Io brightened 15% at 4500 Å following an eclipse by Jupiter. Searches by others, however, (e.g., Ververka et al., 1981) have produced negative results, leading some investigators to conclude that posteclipse brightening on Io does not occur. As an explanation for the phenomenon, Nelson and Hapke (1978) proposed radiation-induced thermoluminescence of surface materials. Irradiation-induced luminescent emissions in salts considered relevant to Io were studied by Nelson and Nash (1979) and found to be small compared with the intensity of reflected solar light. The possibility that ion-irradiated SO_2 frosts may exhibit thermoluminescence is addressed in the present experiment. Previous studies have concentrated on phosphorescence of photostimulated SO_2 at low temperatures (e.g., Meyer et al., 1968).

Several experiments have demonstrated that new molecular species are synthesized as the result of particle irradiation of pure ices or ice mixtures. For example, Berger (1961), Oro (1963), Florin et al. (1962), and Pirronello et al. (1982) detected new molecular products in gases vaporized from irradiated ices during warming or in the nonvolatile residue which remained at room temperature. Moore et al. (1983) observed infrared spectral features of several synthesized molecules in irradiated cometary-type ice mixtures at low temperatures.

In the present investigation it is found that infrared spectra of proton-irradiated SO_2 ice show synthesis of new molecules. The laboratory experiments were designed to reasonably simulate the temperature, pressure, and radiation environment on the surface of Io: the ice temperature was maintained at 80–90°K, the pressure was 10^{-7} torr, and the irradiation varied from

0.01 to 10 ID. Thermoluminescent emissions and visible color changes of the ices were recorded. After each SO_2 ice sample was irradiated, it was warmed to room temperature and the remaining nonvolatile residue was analyzed using infrared or mass spectrometric techniques. Implications of these results for the satellite Io are discussed.

EXPERIMENTAL

The basic experimental arrangement is shown schematically in Fig. 1. A low-temperature, closed-cycle cryostat is attached to an ion-pumped vacuum system and a Van de Graaff accelerator. Ice films were formed by condensing SO_2 gas (purity >99.9%; source, Matheson) onto the gold-coated aluminum mirror attached to the cold finger of the cryostat. The mirror could be maintained at any temperature between 20 and 300°K with a temperature stability of ~0.5°K during the irradiation of the condensed film. The back of the mirror was anodized with sapphire to provide low thermal resistance. Since sapphire also has a high electrical resistance, the mirror is electrically isolated from ground and was used to measure the current resulting from the incident proton beam. A thin foil separated
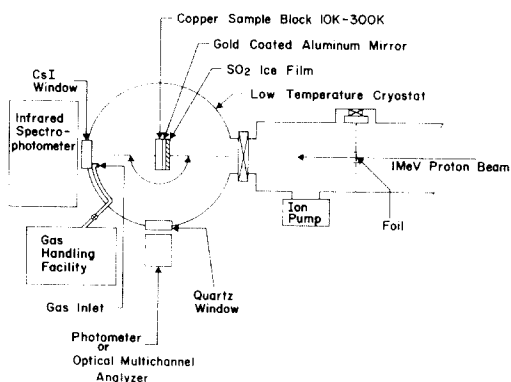

FIG. 1. Arrangement of the spectrophotometer, low-temperature cryostat, and 1-MeV proton beam. An ice film is shown facing the proton beam. Infrared spectra are recorded by rotating the sample 180°; luminescence is measured when the sample faces the quartz window.

the vacuum system of the Van de Graaff accelerator from that of the ion-pumped cryostat to prevent contamination. After passing through the foil, the beam size increased (due to scattering) and the entire 5-cm^2 area of the ice-covered mirror was irradiated. Each proton's energy was reduced ~3% during passage through the foil.

A Perkin–Elmer 621 double-beam spectrophotometer was used to measure the absorption spectrum of the ices over the spectral range 3.3 to 27 μm with a spectral resolution of 3 cm^{-1}. The sample beam from the spectrometer was directed near normal incidence onto the deposited ice. After passing through the sample and being reflected from the gold mirror, the beam (together with the component reflected from the surface of the sample itself) was recombined with the reference beam. Using this arrangement, the spectrum of the ice could be measured at any time during the experiment by rotating the sample in the direction of the infrared beam. Observations of coloration or thermoluminescence were made by rotating the sample to face the quartz window.

The 1-MeV proton source was a High Voltage Corporation Van de Graaff accelerator at the NASA/GSFC. The beam current in these experiments varied from 1.5×10^{-8} to 1.0×10^{-10} A, corresponding to incident proton fluxes of 1.9×10^{10} and 1.2×10^8 cm^{-2} sec^{-1}, respectively (5-cm^2 sample area); in a 2-μm-thick ice film these fluxes result in an absorbed fluence of 1.3–0.009 ID, respectively, in approximately 100 min. The sputtering yield for 1-MeV protons was taken to be ~0.3 SO$_2$ molecules proton^{-1} (Lanzerotti et al., 1982). During laboratory experiments, the fraction of a 2-μm-thick SO$_2$ sample sputtered is 1×10^{-5} and 1×10^{-7} from an absorbed proton fluence equivalent to 1.3 and 0.008 ID, respectively. The eroded fraction will approximately double in value for bombardments at 88°K since the sputtering yield is temperature sensitive.

The absorbed fluence (MeV cm^{-2}) in an ice film was calculated from: incident flux × irradiation time × electronic stopping power × molecular ice density × ice thickness. The electronic stopping power (amount of energy lost per unit distance) for 1-MeV protons, 2×10^{-14} eV cm^2 SO$_2$ molecule^{-1}, was calculated by treating the ice as a dense gas film; in this approximation, the electronic stopping powers for atomic sulfur and oxygen (Anderson and Ziegler, 1977) were combined in a 1 : 2 ratio. By using the density of an SO$_2$ crystal, 1.93 g cm^{-3} (Rudolph, 1977), the penetration range for 1-MeV protons was calculated to be ~17 μm. These results can be rescaled for lower ice densities which may be more typical of SO$_2$ frosts on Io. The ice thickness was determined by observing interference fringes at 2458 cm^{-1} produced by multiple reflections within the SO$_2$ film as it was deposited onto the reflecting gold-coated mirror. A brief discussion of techniques for determining the thickness of SO$_2$ films is given in the Appendix.

Identification of synthesized molecular species was based on numerous reference spectra from the literature. In Fig. 2 the curve labeled Before shows the spectrum of an SO$_2$ ice film at 88°K before irradiation. The fundamentals are identified, and listed in Table I. The 2343 cm^{-1} line due to solid CO$_2$, a contaminant (estimated CO$_2$/SO$_2$ ~ 10^{-3}),was in all mixtures.

In addition to the study of irradiated SO$_2$ ice films, infrared spectra of the following composite samples were measured before and after irradiation: (1) SO$_2$ + sulfur and (2) SO$_2$ + K$_2$S$_2$O$_5$ + Na$_2$S$_2$O$_5$. For the SO$_2$ + sulfur sample, sublimed sulfur (Mallinckrodt) was vacuum deposited from a two-stage furnace onto the gold mirror forming a predominantly octasulfur film with an absorption at 465 cm^{-1} (Bernstein and Powling, 1950). SO$_2$ was deposited at low temperatures on top of the sulfur. For the sulfur + disulfite sample, the disulfite mixture was ground in a mortar, sieved, and electrostatically attracted to the gold mirror. SO$_2$ was deposited at low temperatures
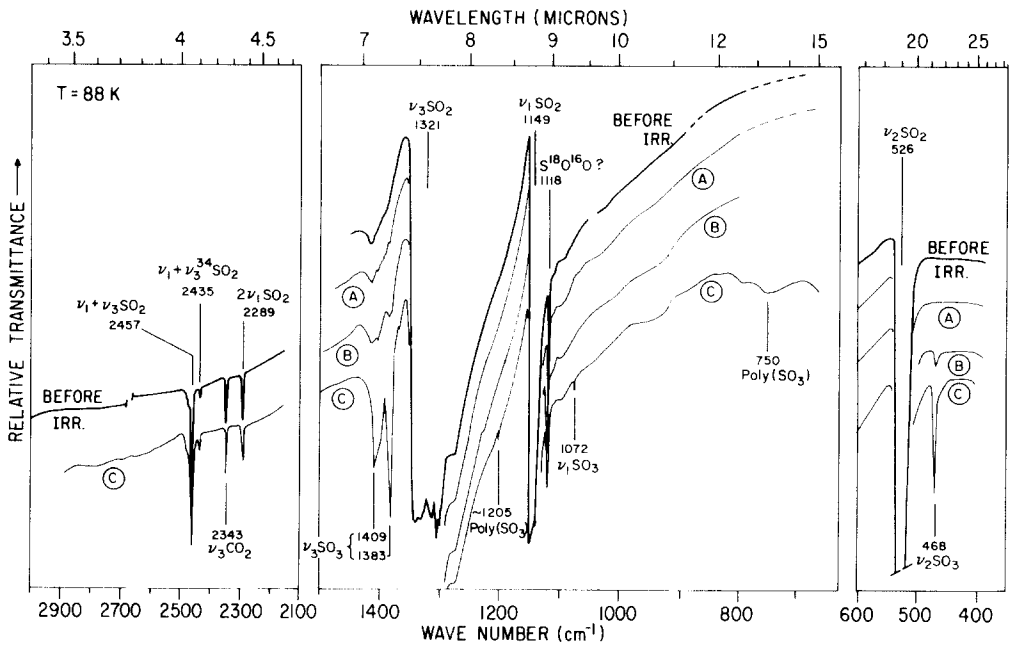
FIG. 2. Infrared transmission spectra of an SO_2 ice (~18 μm thick) at 88°K before and after irradiation with 1-MeV protons. Absorption lines at 1409, 1393, 1072, and 468 cm^{-1} are due to SO_3. Poly(SO_3) is observed near 1200, 865, and 750 cm^{-1}. Curve A is the spectrum after an estimated deposition (eV molecule^{-1}) simulating 0.10 years on Io; curve B simulates 1 year; and curve C simulates 10 years.

on top of this disulfite layer. Color changes in irradiated sulfur (sublimed, Mallinckrodt) pellets were also observed.

After irradiation, the ice temperature was increased at a constant rate using heaters in the cryostat. During warming, thermoluminescence (TL) was visually observed and the integrated intensity for wavelengths shortward of 5500 Å was measured using a 1P28 photomultiplier. The thermoluminescent spectrum was recorded using a Princeton Applied Research Laboratory (Model SSR, 1295A) optical multichannel analyzer (OMA) and a Jarrell Ash (Model 82-410SP) grating monochromator. The monochromator was spectrally calibrated using Hg vapor lines. Emission measurements were corrected for background signals. While warming the ice, pressure changes in the vacuum system were monitored by measuring the ion-pump current. The room temperature residue was analyzed using infrared or mass spectrometric techniques.

RESULTS

A. Molecular Synthesis

Figure 2 shows the infrared spectra of an SO_2 ice sample ~18 μm thick at 88°K before and after irradiation. The major new absorption lines in the spectra after irradiation result from the synthesis of SO_3; the ν_3 fundamental occurs near 1400 cm^{-1}, ν_1 at 1072 cm^{-1}, and ν_2 at 468 cm^{-1}. Polymeric SO_3 is identified with the broad adsorptions near 1205 and 750 cm^{-1}. Positions and identifications of absorption features in the ice are listed in Table I. Reference spectra for SO_2 were obtained from Barbe et al. (1971), G. Sill (1980, personal communication), and R. Khana, M. Ospina, and G. Jere (1983, personal communication); those for SO_3 were obtained from Hopkins et al. (1973), Lovejoy et al. (1962), Bent and Lander (1963), and Jere et al. (1984). Spectra A–C (Fig. 2) demonstrate that more SO_3 is synthesized with increased proton dose (note

TABLE I

WAVENUMBERS OF ABSORPTION FEATURES IN SO$_2$ ICE BEFORE AND AFTER 1-MeV PROTON IRRADIATION

Identification	$T = 88°K$		$T = 20°K$	
	Before irradiation	After irradiation	Before irradiation	After irradiation
$\nu_1 + \nu_3$ SO$_2$	2457		2458	
$\nu_1 + \nu_3$ ^{34}SO$_2$	2435			
ν_3 CO$_2$	2343		2344	
$2\nu_1$ SO$_2$	2289		2293	
ν_3 SO$_3$		1409, 1383		1399, 1385
ν_3 SO$_2$	1321[a]		1319[a]	
Poly(SO$_3$)		1205–1215		1200–1230
ν_1 SO$_2$	1149		1145	
ν_1 S^{16}O^{18}O	1118[b]		1115[b]	
ν_1 SO$_3$		1072		1067
Poly(SO$_3$)		750[c]		840,[c] 758[c]
ν_2 SO$_2$	526		524	
ν_2 SO$_3$		468		462

[a] Center of broad line.
[b] Tentative identification.
[c] Average position.

that each irradiation was at a different dose rate). SO$_3$ is first detected in spectrum B which was recorded after the ice had absorbed ~0.2 eV molecule^{-1}, an amount of energy estimated equivalent to that absorbed by a 17-μm-thick ice on Io in 1 year. The ratio SO$_3$/SO$_2$ is ~0.009. Spectrum C results after continued irradiation to an estimated deposition (~1.9 eV molecule^{-1}), simulating the amount of energy absorbed in a 17-μm-thick ice on Io over 10 years. The ratio SO$_3$/SO$_2$ is ~0.1. These estimates are made by calculating the equivalent thickness of SO$_3$ synthesized using the strength of the unsaturated ν_2 SO$_3$ line and an appropriate absorption coefficient in the standard Lambert–Bouguer radiation law. Preliminary measurements by R. Khanna, M. Ospina, and G. Jere (1983, personal communication) indicate that the ν_2 SO$_3$ fundamental has a peak absorption coefficient of 3000 ± 1000 cm^{-1} (a value of 3000 cm^{-1} was used in this paper).[1] The calculated SO$_3$/SO$_2$, ratio

[1] For comparison, ν_2 SO$_2$ at 90°K has a peak absorption coefficient of 16,000 ± 1000 cm^{-1} (G. Sill, 1980, personal communication).

as a function of absorbed energy, for 10 SO$_2$ ice-irradiation experiments at 88°K showed more scatter than similarly calculated ratios for bombardments at 20°K. Table II summarizes the calculated SO$_3$/SO$_2$ ratio in 17-μm SO$_2$ (the penetration range of a 1-MeV proton) possible on Io as a function of time, based on these experiments. These data, which specifically exclude the effects of removal and burial mechanisms, show that similar synthesis on Io could result in 1% SO$_3$ in a 17-μm layer in 1 year. If it is assumed, however, that SO$_2$ is deposited on the surface of Io at the 1-mm-year^{-1} resurfacing rate estimated by Johnson and Soderblom (1983), then the steady-state abundance of SO$_3$ due to radiation synthesis on Io's surface is reduced to about 0.01%. Table II also gives an estimate of the removal rate of SO$_2$ due to the erosion by plasma ions.

Similar results were observed in films at lower temperatures. Several spectra of SO$_2$ ice at 20°K before and after irradiation are shown in Fig. 3. Positions and identifications of the observed spectral features are also listed in Table I. Each spectrum in Fig.

MARLA H. MOORE

TABLE II

Estimated Rate of 1-MeV Proton Radiation Synthesis of SO_3 on Io (Resurfacing Neglected)

Time (years)	Absorbed fluence (MeV cm^{-2})[a]	Absorbed energy (eV SO_2 molecule^{-1})[b]	SO_3/SO_2	% SO_2 ice (17 μm thick) sputtered on Io[c]
0.1	6.3×10^{11}	0.02	0.0009–0.002[d]	7
0.5	3.2×10^{12}	0.10	0.005–0.01[d]	29
1	6.3×10^{12}	0.19	0.009–0.02	60
5	3.2×10^{13}	0.98	0.05–0.12	100
10	6.3×10^{13}	1.9	0.1–0.2	100

[a] Estimate based on interpretations by Lanzerotti et al. (1982) for 1-MeV protons in 17-μm SO_2 ice.

[b] Assume a 17-μm-thick SO_2 ice, molecular density $= 1.8 \times 10^{22}$ molecules cm^{-3}. These calculations can be rescaled for a different ice density.

[c] Sputtering due to S and O plasma ions: $\sim 7 \times 10^{11}$ SO_2 molecules cm^{-2} sec^{-1} or a surface-loss rate of 10 μm year^{-1} (Johnson et al., 1984). Zero resurfacing rate is assumed.

[d] Estimates based on extrapolation of measured data.

3 was measured using a different SO_2 ice sample, but the initial thickness of each was ~ 24 μm. Spectra A, C, and D (Fig. 3) show that the strength of the SO_3 absorption line increases with increased dose (each irradiation experiment used a different dose rate). Spectra A and B (Fig. 3), however, received different total doses obtained using
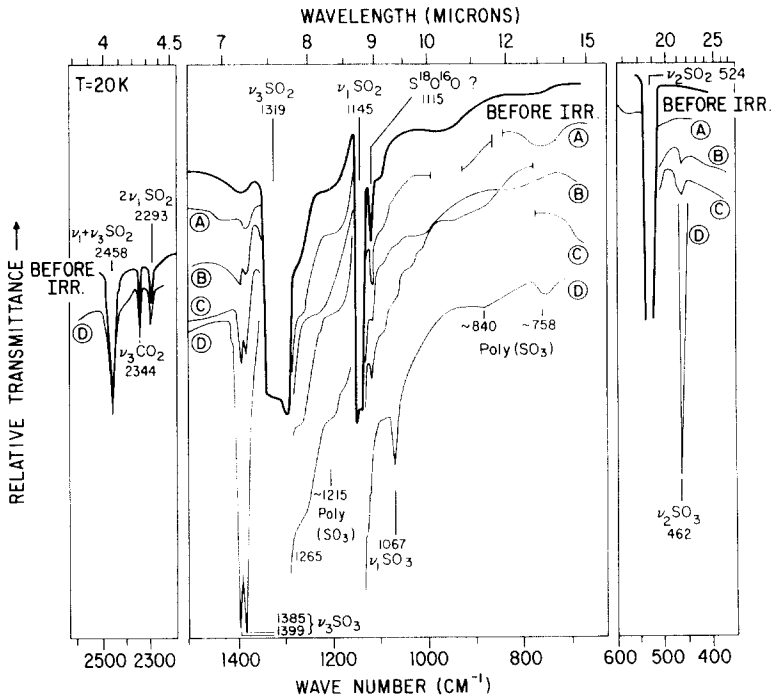

Fig. 3. The infrared transmission spectra of different samples of SO_2 ices (each ~ 24 μm thick) at 20°K before and after irradiation with 1-MeV protons. Absorption lines at 1385, 1399, 1067, and 462 cm^{-1} are due to SO_3. Poly(SO_3) is observed near 1215, 840, and 740 cm^{-1}. Curve A is the spectrum for an absorbed fluence (MeV cm^{-2}) of 5×10^{11} in 100 min; curve B, 2×10^{12} in 6 hr; curve C, 4×10^{12} in 100 min; and curve D, 4×10^{13} in 100 min.

comparable dose rates over different time intervals (100 min and 6 hr, respectively); these spectra suggest that SO_3 synthesis is dependent on total dose and not on the dose rate.

SO_3 signatures between 3.3 and 5 μm (a spectral region of interest to ground-based astronomers) are too weak to be detected in these experiments. In this region the strongest absorption of SO_3 is the $\nu_1 + \nu_3$ fundamental near 2445 cm⁻¹, which lies in the wing of the $\nu_1 + \nu_3$ fundamental of SO_2. Laboratory data by G. Sill (1980, personal communication) demonstrate that sharper SO_2 lines are formed after annealing. Assuming spectra typical of annealed ices, it is estimated that an SO_3/SO_2 ratio of nearly 0.40 may be required before the $\nu_1 + \nu_3$ SO_3 signature could be detected, assuming a 1% noise level.[2] The less intense $2\nu_3$ absorption (~2772 cm⁻¹) was not detected in a relatively unobscured region of the laboratory spectrum.

Synthesis of SO_3 is the major observed effect in irradiated SO_2 ices, and was recorded in more than 20 ice films of different thicknesses. Synthesis occurred in ices <17 μm thick (in these, 1-MeV protons penetrate the ice and come to rest in the gold mirror) and in ices 17–150 μm thick (in these, all protons are stopped in the ice). SO_3 synthesis was also observed in irradiated composite samples which were selected as examples of possible Ionian-type surface materials. These were SO_2 ice over a layer of sulfur and SO_2 ice over a mixture of powdered sodium and potassium disulfites. Spectra of sulfur + SO_2 are shown before and after irradiation in Fig. 4a. The thickness of the sulfur was estimated to be 30–40 μm (an absorption coefficient of 100 cm⁻¹ for 2 ν_7 S_8 at 465 cm⁻¹ appears con-

[2] This estimate was made using two Lorentzian line profiles of equal FWHM, one for $\nu_1 + \nu_3$ SO_2 (peak absorption coefficient at 2457 cm⁻¹ = 1800 cm⁻¹ (G. Sill, 1980, personal communication) and one for $\nu_1 + \nu_3$ SO_3 (peak absorption coefficient at 2445 cm⁻¹ estimated to be 180 cm⁻¹ (R. Khanna, M. Ospina, and G. Jere, 1983, personal communication).
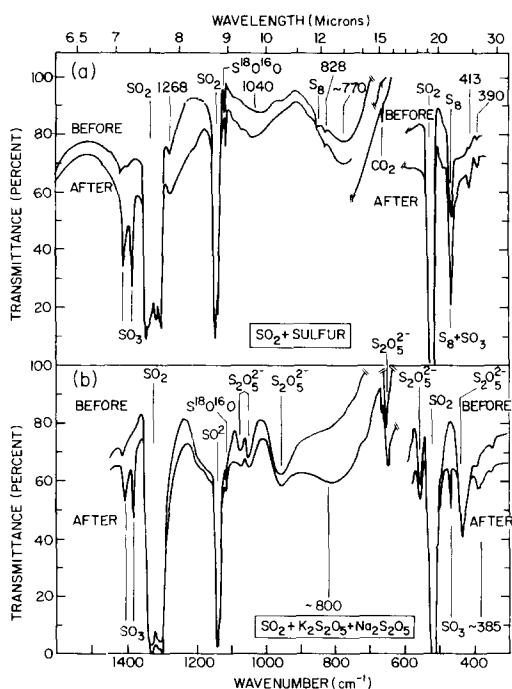

FIG. 4. Infrared transmission spectra of composite samples containing SO_2 at 80°K before and after irradiation with 1-MeV protons. Synthesis of SO_3 is demonstrated by the presence of lines at 1408, 1381, and 468 cm⁻¹. (a) Spectra of SO_2 + S_8. Absorbed fluence in the (~19 μm thick) SO_2 layer was ~10¹³ MeV cm⁻². The S_8 layer was 30–40 μm thick. (b) Spectra of SO_2 + $K_2S_2O_5$ + $Na_2S_2O_5$. Absorbed fluence in the (~9 μm thick) SO_2 layer was 10¹³ MeV cm². The thickness of the disulfite layer was not determined. See Table III for identification of spectral features.

sistent with the data of MacNeill (1963)); the thickness of the SO_2 film deposited on top of the sulfur was estimated to be near 19 μm. The synthesis of SO_3 and polymeric SO_3 was observed as a result of irradiation. Spectra of SO_2 + $K_2S_2O_5$ + $Na_2S_2O_5$ are shown before and after irradiation in Fig. 4b. Absorptions attributed to the disulfites appear stable against proton irradiation. SO_3 is synthesized in the 9-μm-thick SO_2 ice during irradiation. Line positions and identification of spectral feature in Fig. 4 are listed in Table III.

B. Thermoluminescence

During slow warming (after irradiation of the SO_2 ice was completed), thermolumi-

TABLE III

Positions of Absorption Features in Composite Samples (Fig. 4) before and after Irradiation (T = 80°K)

Figure	Identification	Line or band position (cm^{-1})	
		Before irradiation	After irradiation
	Interference pattern[a]	1350, 1040, 770	
4a	$\nu_3 SO_3$		1408, 1381
	$\nu_3\ SO_2$	1321	
	1268, Un[b]	1268	
SO$_2$ + sulfur	$\nu_1\ SO_2$	1149	
	$\nu_1\ S^{16}O^{18}O$	1118[a]	
	$\nu_3 S_8$[c]	848	
	828, Un[b]	828	
	$\nu_2\ CO_2$	660	
	$\nu_2\ SO_2$	526	
	$\nu_2\ SO_3$		468
	$2\ \nu_7\ S_8$[a,c]	465	
	413, Un[b]	413	
	390, Un[b]	390	
	$\nu_3\ SO_3$	1408, 1381	
	ν_3 and $\nu_1\ SO_2$	1321,[d] 1149	
	$\nu_1\ S^{16}O^{18}O$	1118[a]	
	$\nu_1, \nu_2, \nu_3\ (S_2O_5^{2-})$[e]	1079, 1050, 965	
	790, H$_2$O		790
	$\nu_4(S_2O_5^{2-})$[e]	655	
4b	$\nu_2\ SO_2$	526	
SO$_2$ + K$_2$S$_2$O$_5$ +	$\nu_2\ SO_3$		468
Na$_2$S$_2$O$_5$	$\nu_7(S_2O_5^{2-})$[e]	435	
	385, Un[b]		385

[a] Tentative identification.
[b] Unidentified.
[c] Bernstein and Doweling (1950).
[d] Center of broad line.
[e] Meyer et al. (1980).

nescence (TL) was visually observed and photometrically recorded. Figure 5 shows the TL intensity as a function of temperature for several experiments. The absolute luminescent intensity was estimated using the appropriate geometrical viewing factor and detector quantum efficiency. Curves A–D are the emissions from 20°K irradiated SO$_2$ ices during warming from 20 to 200°K (warming rate 10°/min). The most intense luminescent emission occurs near 40°K; weaker emission is observed in all samples as the ice is warmed to 80°K. The 155°K enhancement can be associated with the vaporization of SO$_2$ ice. Luminescence measured immediately after irradiation, without warming (termed afterglow, AG), was also observed in an SO$_2$ ice at 20°K. The afterglow intensity decayed an order of magnitude in 30 min (intensity AG ≪ intensity TL). Curve F is the result of a control experiment (unirradiated SO$_2$); the observed emission near 150°K resulted from light scattered from the ionization region of the ion pump during small pressure enhancements caused by the vaporizing ice. The emission at 25°K probably results from a pressure enhancement caused by the release of SO$_2$ from a region of the cryostat warmed above 150°K by the heaters.

To more closely simulate the thermal environment on Io's surface during an

SO₂ ICE IRRADIATED AT 20 K

ABSORBED FLUENCE (MeV-cm⁻²)

- A. 6.1×10^{13}
- B. 4.4×10^{12}
- C. 2.8×10^{12}
- D. 5.9×10^{11}
- F. BACKGROUND(SO₂ ICE-NO IRR)

SO₂ ICE IRRADIATED AT 88 K

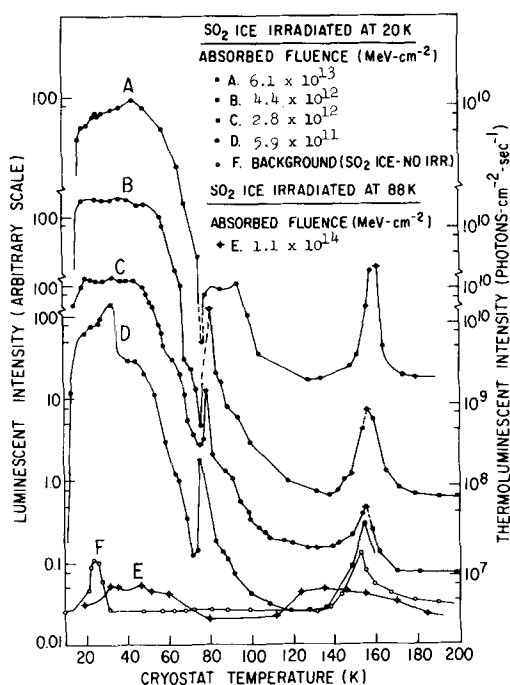ABSORBED FLUENCE (MeV-cm⁻²)

- E. 1.1×10^{14}

FIG. 5. Intensity of thermoluminescent emissions as a function of temperature during warming of SO₂ ices irradiated at 20°K (curves A–D), and at 88°K (curve E). Curve F is a background signal recorded during warming unirradiated SO₂ ice (a control sample).

eclipse, a similar luminescence experiment was carried out with an SO₂ ice irradiated at 88°K. After recooling the irradiated sample to 20°K, for convenience, thermoluminescent emissions are shown in curve E. The area under curve E (20–80°K) is 1/70,000 the area under the large emission curve A (20–80°K).

The luminescence spectrum of an SO₂ ice film irradiated at 20°K (absorbed fluence 4 × 10¹² MeV cm⁻²) was measured during warming from 20 to 60°K. Within the range of the monochromator (3280 to 6300 Å), a single emission peak (FWHM = 460 Å) was observed at 4450 Å. The ion pump was closed during this experiment to prevent the detection of any light emitted from its ionization region.

C. Color Changes

SO₂ films a few microns in thickness ap-

pear transparent, whereas those >100 μm in thickness appear white in color after deposition at 88 or 20°K probably because they are not a smooth compact ice but a less dense film. At 88°K, proton irradiated SO₂ films become light yellow after fluences simulating approximately 1 ID (10¹³ MeV cm⁻²); after a fluence simulating approximately 10 ID the film is darker yellow. Ultraviolet and visible spectral studies of the stability of these colors as a function of temperature is in progress.

Frosts of SO₂ at 20°K, (thickness > 100 μm) turned yellow and then dark orange after absorption of 10¹⁴ and 10¹⁵ MeV cm⁻², respectively. An abrupt color change from dark orange to light yellow-orange was observed at 32°K when the underlying mirror temperature was slowly increased.

Pressed sulfur samples were white when cooled to 88 or 20°K. Sulfur irradiated at 88°K formed dark orange-brown and dark brown areas after irradiation to approximately 10 ID. Sulfur irradiated at 20°K exhibited a greater variety of colors (black, violet, blue-green, and dark brown) which are apparently due to the formation of various sulfur allotropes (Meyer, 1977). The large variety of colors across a single sample might result from spatial nonuniformities in proton beam intensity and/or variations in the integrity of the pressed sulfur (sometimes the sample flaked and exhibited colorations which changed at distinct rather than diffuse boundaries). Colors of sulfur irradiated at 20°K changed when the temperature was increased; for example, when warmed to 144°K sulfur samples were black-brown-dark brown and this coloration changed to dark yellowish brown as the temperature approached 250°K. At room temperature irradiated sulfur samples returned to their original yellow color. These observations were made visually through the cryostat window and are only mentioned here to indicate the complex nature of irradiated sulfur; they are not intended to be quantitative. Radiation-induced color changes have also been observed using other types of ionizing radi-
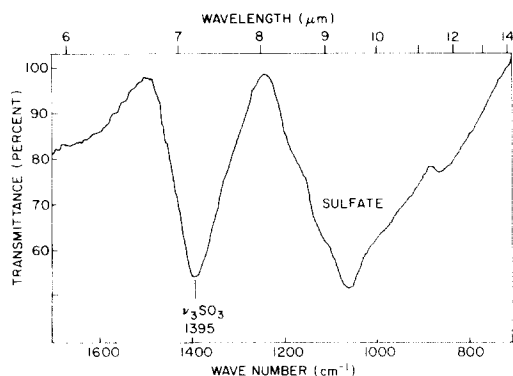
FIG. 6. Infrared transmission spectrum of a typical residue present after warming an irradiated SO_2 ice to room temperature. The β form of SO_3 is identified with the 1395 cm^{-1} absorption. The band near 1050 cm^{-1} suggests the presence of a sulfate. S_8, detected using mass spectroscopy, is not observed in the spectrum $(2\nu_7, 465$ cm$^{-1})$ because of its relatively small abundance and low absorption coefficient.

ation (reviews by Meyer, 1977; Nelson and Nash, 1978). The stability of colors in irradiated sulfur with temperature and time needs to be addressed in detail (Sagan, 1979).

D. Residue

Infrared spectra showed the development of several complex, temperature-dependent bands which shifted position and changed intensity when irradiated SO_2 ices were warmed. These features are apparently due to various polymers of SO_3. A study of the infrared features of SO_3 as a function of temperature is discussed by Jere et al. (1984). At room temperature (in all experiments) a yellowish nonvolatile residue was found on the mirror. The spectrum of a typical residue is shown in Fig. 6. The absorption features are identified as the β form of SO_3 and a sulfate. The sulfate is likely to be aluminum sulfate, formed in pits or at the edges of the gold film covering the aluminum substrate. Infrared spectra of similarly formed residues on aluminum closely matched the spectra of aluminum sulfate and showed no SO_3 signatures. In a separate experiment a similar residue was

irradiated at 20°K (1 ID), and the resulting infrared spectrum was unchanged, indicating a degree of stability against radiation. When the SO_3 and sulfate fractions were removed with water, a hazy residue was still present on the mirror. This hazy film showed no detectable infrared absorption features. In a separate experiment, mass spectrographic analysis of the entire residue was used to identify SO_3 and S_8.

DISCUSSION

The synthesis of SO_3 was the dominant result for all irradiation experiments on SO_2 ices at 88 and 20°K, including composite samples of SO_2 ice over S_8 and over $K_2S_2O_5$ + $Na_2S_2O_5$ powder. Based on these laboratory simulations, it is predicted that Jovian magnetospheric radiation will synthesize SO_3 in the upper SO_2 ice layers on Io. The infrared signatures of synthesized molecules (SO_3 and polymeric SO_3) at 88°K during proton irradiation simulations are identified in Table I. The intensity of the ν_2SO_3 absorption feature was a measure of the quantity synthesized (given a film thickness and absorption coefficient), and was used to calculate the SO_3/SO_2 ratio as a function of adsorbed fluence. Table II shows the percentage of SO_3 synthesized in the top 17 μm of ice (the range of a 1-MeV proton) on Io as a function of time based on these laboratory simulations. In 1 year on Io, for example, approximately 1% SO_3 can be synthesized in the top 17 μm layer of SO_2 ice.

The estimates listed in Table II assume unimpeded access of 1-MeV protons to Io's surface and exclude SO_2 and SO_3 removal and burial mechanisms. An order of magnitude estimate of the effects of burial by plume material can be made assuming an SO_2 deposition rate of 1 mm year^{-1} or ~17 μm of new SO_2 frost in ~6 days (Johnson and Soderblom, 1983). Under these conditions, the column density of synthesized SO_3 reaches an equilibrium value 0.01% that of SO_2 in 6 days. This amount of expected

SO$_3$ synthesis is comparable with the 10^{-4}–10^{-6} SO$_3$/SO$_2$ ratio predicted using thermodynamic models of Ospina (1983). If, however, a patch of SO$_2$ frost was in a region with very low burial then the SO$_3$/SO$_2$ ratio could increase toward 1% in the top 17-μm layer in 1 year; within this region, radiation synthesis would be the dominant formation mechanism for SO$_3$. A detailed chemical model of the dynamic surface of Io needs to include removal (burial, sputtering, vaporization, and chemical reactions) and production (radiation synthesis and the fraction from volcanic effluents) mechanisms, a problem not considered in this paper.

Higher energy protons will synthesize SO$_3$ in deeper layers but the rate of synthesis will be less due to the exponential decrease in the differential energy spectrum of protons for $E > 2$ MeV. Low-energy S and O plasma ions ($E < 6$ keV) appear to dominate the measured energetic ion spectrum in the torus. Laboratory irradiations of SO$_2$ ices with heavy ions have also resulted in the synthesis of SO$_3$ (Boring $et\ al.$, 1983; Johnson and Soderblom, 1983); the altered material is in the top few molecular layers of the ice due to the small penetration depths of heavy ions. The flux of 1-MeV electrons (estimated to be the order of 100 times that of 1-MeV protons) also contributes to the energy deposition in Io's ice. The energy of 1-MeV electrons is deposited almost uniformly with depth, over a range $\sim$200 times that of a 1-MeV proton. Since all kinds of ionizing radiation have the same effect at the molecular level, the inclusion of all these energetic particles would increase the expected synthesis rate of SO$_3$ on Io (in the presence of resurfacing at 1 mm year^{-1}) from $\sim$0.01 to $\sim$0.04% in the top 17-μm layer of ice. At depths beyond 3 mm (the approximate penetration range of a 1-MeV electron), an equilibrium column density of SO$_3$ would be reached in approximately 3 years at a value several percent that of SO$_2$.

The peak thermoluminescent intensity measured for SO$_2$ ices irradiated by 1-MeV protons at 20K was at least 2000 times greater than that for ices irradiated at 88°K. Thermoluminescence is thought to result from mechanisms such as the electronic relaxation of excited SO$_2$ molecules (Meyer $et\ al.$, 1968) or the radiative recombination of trapped electrons and cations. Radiation-induced excited species trapped at temperatures near 20°K can react when the sample is warmed. At 80°K, the storage of excited species becomes less efficient due to increased diffusion within the ice and this results in diminished luminescent intensity during warming. These experiments did not provide enough information to determine the mechanism responsible for either the main low-temperature thermoluminescent emissions or the secondary emissions near 80°K. Analysis of luminescent curves (curves A–D; Fig. 5) as a function of temperature ($T < 40$°K) yields an activation energy, E, of $\sim$0.05 eV. The initial rise in luminescent intensity is given by

$$I = Ae^{-E/kT},$$

where E is the activation energy, k is the Boltzman constant, and T is the absolute temperature (see, e.g., Garlick and Gibson, 1948). A similar activation energy value was calculated for proton-irradiated cometary-type ice mixtures containing water at 20°K (Moore, 1981).

The thermoluminescent spectrum peaked at 4450 Å, a value similar to that of the emission envelope maximum of the phosphorescent spectrum (spectrum measured during photon stimulation) of matrix isolated SO$_2$ (Phillips $et\ al.$, 1969; Meyer $et\ al.$, 1968). The thermoluminescent intensity and spectral data from irradiated SO$_2$ ices were combined to estimate that the contribution to posteclipse brightening of similar luminescence on Io would be 10^{-7} to 10^{-9} times the flux from reflected sunlight; thus, thermoluminescence from SO$_2$ ice excited by 1-MeV protons would be an insignificant contributor to any posteclipse brightening phenomena.

Based on the present experiment, Jovian magnetospheric irradiation of SO_2 frost on Io synthesizes SO_3. If SO_2 frost is locally sublimated by solar or subsurface heating at a greater rate than it is supplied by resurfacing, a low-volatility residue containing a form of SO_3, S_8, and possibly a sulfate will remain on the surface. The sputtering rate of a similar laboratory synthesized residue (observed to be oxygen rich relative to sulfur) was estimated to be an order of magnitude less than the rate for SO_2 (Melcher et al., 1982). Since SO_3 is more stable against removal mechanisms (sublimation and sputtering) than SO_2, and is an extremely reactive molecule, it may play a role in determining the types of materials present on Io's surface, which in turn affects the amount of material sputtered from the surface into the atmosphere or torus.

SUMMARY

1. SO_3 is the dominant molecular species synthesized in SO_2 ice as a result of 1-MeV proton irradiation at 20 or 88°K. Polymeric SO_3 is also identified at low temperatures.

2. In the absence of resurfacing, similar SO_3 synthesis on Io could result in SO_3/SO_2 $\cong 0.01$ to as much as ~0.1 in 17-μm surface layers after 1 to 10 years, respectively, after irradiation of 88°K SO_2 surface frost by Jovian magnetospheric 1-MeV protons. At a resurfacing rate of 1-mm-year^{-1} SO_3/SO_2 would be reduced to ~10^{-4}.

3. During warming of irradiated SO_2 ice at 20°K, thermoluminescence occurs (λ peak = 4450 Å) which is most intense between 15 and 70°K. Thermoluminescence from SO_2 irradiated at 88°K is at least 2000 times less intense than that from 20°K irradiated ices. Emissions from such a phenomenon on Io would not be measurable during posteclipse observations.

4. SO_2 ice was observed to change from white to light yellow in color after irradiation with 1-MeV protons at 20 and 88°K. Sulfur pellets were observed to darken and exhibit a range of colors after proton irradi-

ation at 88°K, and to return to their original yellow color after warming to 300°K.

5. A nonvolatile residue containing a form of SO_3, sulfate, and S_8 is present at 300°K after warming the irradiated SO_2 ice.

APPENDIX

The physical thickness of SO_2 films, d, deposited at 20°K was calculated using the relation:

$$d = \frac{m\lambda}{2n},$$

where m is the number of growth fringes measured during deposition at $\lambda = 4.07$ μm (2458 cm^{-1}, the center of the $\nu_1 + \nu_3$ absorption line), and n is the index of refraction of the film which was estimated using the standard Kramers–Kronig analysis (J. Pearl, 1983, personal communication) for an absorption coefficient measured for SO_2 at 90°K (G. Sill, 1980, personal communication). If the ice thickness is obtained by fitting the peak intensity of the 2458 cm^{-1} line of SO_2 using the standard Lambert–Bouguer radiation law and the measured absorption coefficient (G. Sill, 1980, personal communication), the physical thickness is almost five times smaller than that determined by the growth fringe technique. Sill, however, measured the absorption coefficients of SO_2 at 90°K (after annealing the ice at 130°K). The discrepancy appears to be due to the large difference in the peak intensity of absorption lines of films deposited at different temperatures, different rates, and with different histories.

REFERENCES

ANDERSON, H. H., AND J. F. ZEIGLER (1977). *Hydrogen, Stopping Powers and Ranges in All Elements*. Pergamon, New York.

BARBE, A., A. DELAHAIGUE, AND P. JOUVE (1971). Spectre infrarouge a letat solide des molecules isotopiques de SO₂. *Spectrochimica Acta* **27A**, 1439–1446.

BENT, R., AND W. R. LANDER (1963). The infrared spectrum of gaseous sulfur trioxide. *Spectrochemica Acta* **19**, 931–935.

BERGER, R. (1961). The proton irradiation of methane, ammonia and water at 77K. *Proc. Natl. Acad. Sci. USA* **47**, 1434–1436.

BERNSTEIN, H. J., AND J. POWLING (1950). The vibrational spectra and structure of inorganic molecules. *J. Chem. Phys.* **18**, 1018–1023.

BERTAUX, J. L., AND M. J. S. BELTON (1979). Evidence of SO₂ on Io from UV observations. *Nature* **282**, 813–815.

BINDER, A. B., AND D. P. CRUIKSHANK (1964). Evidence for an atmosphere on Io. *Icarus* **3**, 299–305.

BORING, J. W., J. W. GARRETT, E. SIEVEKA, AND R. E. JOHNSON (1983). Sputter-induced atmosphere and molecular ejection on Io. *Lunar Planet. Sci. Conf. 14th.*

BRIDGE, H. S., J. W. BELCHER, A. J. LAZARUS, J. O. SULLIVAN, R. A. MCNUTT, F. BAGENAL, J. D. SCUDDER, G. C. SITTLER, G. L. SISCOE, V. M. VASYLIUNAS, C. K. GOERTZ, AND C. M. YEATES (1979). Plasma observations near Jupiter: Initial results from Voyager 1. *Science* **204**, 987–991.

BROWN, R. A. (1974). Optical line emission from Io. *IAU Symp. 65: Exploration of the Planetary System* (A. Woszczyk and C. Iwaniszewska, Eds.), pp. 527–531. Reidel, Dordrecht.

BUTTERWORTH, P. S., J. CALDWELL, V. MOORE, T. OWEN, A. R. RIVOLO, AND A. L. LANE (1980). An upper limit to the global SO₂ abundance on Io. *Nature* **285**, 308–309.

DIVINE, N., AND H. B. GARRETT (1983). Charged particle distributions in Jupiter's magnetosphere. *J. Geophys. Res.* **88**, 6889–6903.

FANALE, F. P., R. H. BROWN, D. P. CRUIKSHANK, AND R. N. CLARK (1979). Significance of absorption features in Io's IR reflectance spectrum. *Nature* **280**, 761–763.

FLORIN, R. E., D. W. BROWN, AND L. A. WALL (1962). γ-Irradiation of small molecules at 4 and 77K. *J. Chem. Phys.* **66**, 2672–2677.

GARLICK, G. F. J., AND A. F. GIBSON (1948). The electron trap mechanism of luminescence in sulphide and silicate phosphors. *Proc. Phys. Soc.* **60**, 574–590.

HOPKINS, A. G., S. TANG, AND C. W. BROWN (1973). Infrared and Raman spectra of the low-temperature products from discharged sulfur dioxide. *J. Amer. Chem. Soc.* **95**, 3486–3490.

JERE, G. V., R. K. KHANNA, M. J. OSPINA, AND J. C. PEARL (1984). Sulfur trioxide, a "true chemical chameleon": IR Studies 12K–290K. Submitted for publication.

JOHNSON, R. E., J. W. GARRETT, J. W. BORING, L. A. BARTON, AND W. L. BROWN (1984). Erosion and modification of SO₂ ice by ion bombardment of the surface of Io. Submitted for publication.

JOHNSON, T. V., AND L. A. SODERBLOM (1983). Volcanic eruptions on Io: Implications for surface evolution and mass loss. In *Satellites of Jupiter* (D. Morrison, Ed.), pp. 634–646. Univ. of Arizona Press, Tucson.

KRIMIGIS, S. M., R. P. ARMSTRONG, W. I. AXFORD, C. O. BOSTROM, C. Y. FAN, G. GLOECKLER, L. J. LANZEROTTI, E. P. KEATH, R. C. ZWICKL, J. P. CARBARY, AND D. C. HAMILTON (1979). Hot plasma environment at Jupiter: Voyager 2 results. *Science* **206**, 977–984.

LANZEROTTI, L. J., W. L. BROWN, W. M. AUGUSTYNIAK, R. E. JOHNSON, AND R. P. ARMSTRONG (1982). Laboratory studies of charged particle erosion of SO₂ ice and applications to the frosts on Io. *Astrophys. J.* **259**, 920–929.

LOVEJOY, R. W., J. H. COLWELL, D. F. EGGERS, JR., AND G. O. HALSEY, JR. (1962). Infrared spectrum and thermodynamic properties of gaseous sulfur trioxide. *J. Chem. Phys.* **36**, 612–617.

MACNEILL, C. (1963). Infrared transmittance of rhombic sulfur. *J. Opt. Soc. Amer.* **53**, 398–399.

MELCHER, C. L., D. J. LEPOIRE, B. H. COOPER, AND T. A. TOMBRELLO (1982). Erosion of frozen sulfur dioxide by ion bombardment: Application to Io. *Geophys. Res. Lett.* **9**, 1151–1154.

MEYER, B. (1977). *Sulfur, Energy and the Environment*, pp. 429–451. Elsevier, Amsterdam.

MEYER, B., M. OSPINA, AND C. PETER (1980). *Anal. Chem.* **117**, 301–308.

MEYER, B., L. F. PHILLIPS, AND J. J. SMITH (1968). Temperature dependence of intersystem crossing: Lifetime and intensity of SO₂ phosphorescence in low temperature solids. *Proc. Natl. Acad. Sci. USA* **61**, 7–11.

MOORE, M. H. (1981). *Studies of Proton-Irradiated Cometary-type Ice Mixtures*. Ph.D. thesis, University of Maryland, College Park.

MOORE, M. H., B. DONN, R. KHANNA, AND M. F. A'HEARN (1983). Studies of proton-irradiated cometary-type ice mixtures. *Icarus* **54**, 388–405.

NASH, D. B., AND F. P. FANALE (1977). Io's surface composition based on reflectance spectra of sulfur/salt mixtures and proton-irradiation experiments. *Icarus* **31**, 40–80.

NELSON, R. M., AND B. W. HAPKE (1978). Possible correlation of Io's posteclipse brightening with major solar flares. *Icarus* **33**, 203–209.

NELSON, R. M., A. L. LANE, D. L. MATSON, F. P. FANALE, D. B. NASH, AND T. V. JOHNSON (1980).

Io: Longitudinal distribution of sulfur dioxide frost. *Science* **210**, 784–786.

NELSON, R. M., AND D. B. NASH (1978). Radiation induced color changes in proposed Io surface materials. *Bull. Amer. Astron. Soc.* **10**, 580.

NELSON, R. M., AND D. B. NASH (1979). Spectral reflectance change and luminescence of selected salts during 2–10 KeV proton bombardment: Implications for Io. *Icarus* **33**, 277–285.

ORO, J. (1963). Synthesis of organic compounds by high-energy electrons. *Nature* **197**, 971–974.

OSPINA, M. J. (1983). Numerical results on the crustal composition of Io. *IAU Colloq. No. 77: Natural Satellites*. Ithaca, N.Y.

PASCARD, P. R., AND C. PASCARD-BILLY (1965). Structure précise de l'anhydride sulfurique. *Acta Crystallogr.* **18**, 830–834.

PEARL, J., R. HANEL, V. KUNDE, W. MAGUIRE, K. FOX, S. GUPTA, C. PONNAMPERUMA, AND F. RAULIN (1979). Identification of gaseous SO_2 and new upper limits for other gases on Io. *Nature* **280**, 755–758.

PHILLIPS, L. F., J. J. SMITH, AND B. MEYER (1969). The ultraviolet spectra of matrix isolated disulfur monoxide and sulfur dioxide. *J. Mol. Spec.* **29**, 230–243.

PIRRONELLO, V., W. L. BROWN, L. J. LANZEROTTI, K. J. MARCANTONIO, AND E. SIMMONS (1982). Formaldehyde formation in a H_2O/CO_2 ice mixture under irradiation by fast ions. *Astrophys. J.* **262**, 636–640.

RUDOLPH, R. N. (1977). *Spectroscopy and Emission Lifetimes of Sulfur Dioxide*. Ph.D. thesis, University of Colorado, Boulder.

SAGAN, C. (1979). Sulphur flows on Io. *Nature* **280**, 750–753.

SMYTHE, W. D., R. M. NELSON, AND D. B. NASH (1979). Spectral evidence for SO_2 frost or adsorbate on Io's surface. *Nature* **280**, 766.

TRAFTON, L. (1975). Detection of a potassium cloud near Io. *Nature* **258**, 690–692.

TRAINOR, J. H., F. B. MCDONALD, AND B. J. TEEGARDEN (1974). Energetic particles in the Jovian magnetosphere. *J. Geophys. Res.* **79**, 3600–3613.

VEVERKA, J., D. SIMONELLI, AND P. THOMAS (1981). Voyager search for posteclipse brightening on Io. *Icarus* **47**, 60–74.

WAMSTECKER, W., R. L. KROES, AND J. A. FOUNTAIN (1974). On the surface composition of Io. *Icarus* **23**, 417–427.